

Overview of CFD numerical methods

Remark: foils with „black background“ can be skipped, they are aimed to the more advanced courses

CFD and PDE

CFD problems are described by transport partial differential equations (PDE) of the second order (with second order derivatives). These equations describe transport of mass, species, momentum, or thermal energy. Result are temperature, velocities, concentrations etc. as a function of x,y,z and time t

PDE of second order are classified according to signs of coefficients at highest derivatives of dependent variable Φ (for more details, see next slides):

➤ **Hyperbolic equations** (evolution, typical for description of **waves**, finite speed of information transfer)

$$\frac{\partial^2 \Phi}{\partial t^2} - \frac{\partial^2 \Phi}{\partial x^2} = f$$

$$\frac{\partial \Phi}{\partial t} + c \frac{\partial \Phi}{\partial y} = 0$$

convection by velocity c

Examples: supersonic flow around a plane, flow in a Laval nozzle, pulsation of gases at exhaust or intake pipes

➤ **Parabolic equations** (evolution problems, information is only in the direction of evolution variable t - usually time but it could be also distance from the beginning of an evolving boundary layer)

$$\frac{\partial \Phi}{\partial t} + \frac{\partial^2 \Phi}{\partial x^2} = f$$

Examples: evolution of boundary layer (in this case t - represents spatial coordinate in the direction of flow and x is coordinate perpendicular to the surface of body)

➤ **Elliptic equations** (typical for stationary problems, infinite speed of information transfer)

$$\frac{\partial^2 \Phi}{\partial y^2} + \frac{\partial^2 \Phi}{\partial x^2} = f$$

$$\nabla \cdot (\vec{u}\Phi) - a\nabla^2 \Phi + S = 0$$

Examples: subsonic flows around bodies (spheres, cylinders), flow of incompressible liquids

CFD and PDE

Why is it important to distinguish types of PDE?

Because different methods are suitable for different types (e.g. central differencing in elliptical region and **time marching** schemes in hyperbolic or parabolic regions)

Characteristics (1/3)

Type of PDE of the second order (hyperbolic, parabolic, elliptic) is closely related to the notion of characteristics. What is the characteristic of PDE, written for simplicity only as the 2D case (only x,y coordinates, the 3D case is analogical)

$$a \frac{\partial^2 \Phi}{\partial x^2} + b \frac{\partial^2 \Phi}{\partial x \partial y} + c \frac{\partial^2 \Phi}{\partial y^2} = f$$

?

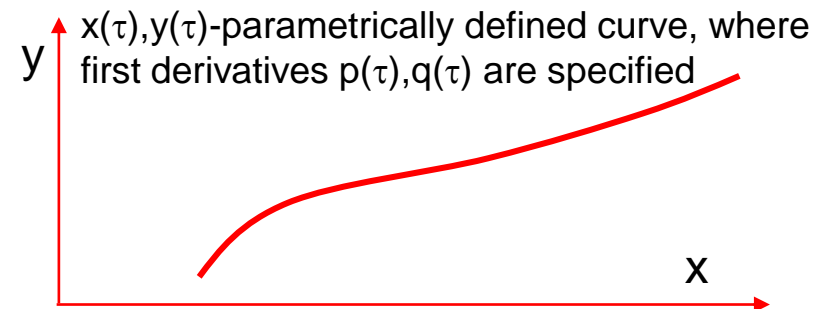
f can be function of x,y,Φ and first derivatives.

Fact: if all Φ values and all first derivatives $\partial\Phi/\partial x, \partial\Phi/\partial y$ are prescribed along an arbitrary curve, it is possible to evaluate all second order derivatives $\partial^2\Phi/\partial x^2, \partial^2\Phi/\partial y^2, \partial^2\Phi/\partial x\partial y$ using the differential equation. Let us assume that the curve is expressed in the parametric form $x(\tau), y(\tau)$ and that the specified first derivatives are also expressed in parametric form $\partial\Phi/\partial x = p(\tau), \partial\Phi/\partial y = q(\tau)$.

Then

$$\frac{\partial p}{\partial \tau} = \frac{\partial p}{\partial x} \frac{\partial x}{\partial \tau} + \frac{\partial p}{\partial y} \frac{\partial y}{\partial \tau} = \frac{\partial^2 \Phi}{\partial x^2} \frac{\partial x}{\partial \tau} + \frac{\partial^2 \Phi}{\partial x \partial y} \frac{\partial y}{\partial \tau}$$

$$\frac{\partial q}{\partial \tau} = \frac{\partial q}{\partial x} \frac{\partial x}{\partial \tau} + \frac{\partial q}{\partial y} \frac{\partial y}{\partial \tau} = \frac{\partial^2 \Phi}{\partial y^2} \frac{\partial y}{\partial \tau} + \frac{\partial^2 \Phi}{\partial x \partial y} \frac{\partial x}{\partial \tau}$$



Characteristics (2/3)

These equations can be expressed in matrix form as

$$\begin{pmatrix} a & b & c \\ \frac{\partial x}{\partial \tau} & \frac{\partial y}{\partial \tau} & 0 \\ 0 & \frac{\partial x}{\partial \tau} & \frac{\partial y}{\partial \tau} \end{pmatrix} \cdot \begin{pmatrix} \frac{\partial^2 \Phi}{\partial x^2} \\ \frac{\partial^2 \Phi}{\partial x \partial y} \\ \frac{\partial^2 \Phi}{\partial y^2} \end{pmatrix} = \begin{pmatrix} f \\ \frac{\partial p}{\partial \tau} \\ \frac{\partial q}{\partial \tau} \end{pmatrix}$$

Right hand side is fully determined by prescribed first derivatives (by boundary conditions) along selected curve

This system can be solved under “normal” circumstances (for almost any selected curve) giving continuous second derivatives as a function of specified “boundary” conditions (prescribed first derivatives). However, as soon as determinant of previous system is zero (and it depends upon a,b,c coefficients of PDE and upon the selected curve), the system is indefinite and second derivatives are not unique and continuous. At these particular curves something happens with the solution. And just these curves are characteristic lines (surfaces at 3D problem), passing through an arbitrary point x,y,z . From the requirement of zero determinant immediately follows

$$a\left(\frac{\partial y}{\partial \tau}\right)^2 - b\frac{\partial x}{\partial \tau}\frac{\partial y}{\partial \tau} + c\left(\frac{\partial x}{\partial \tau}\right)^2 = 0 \quad \text{and}$$

$$a\left(\frac{\partial y}{\partial x}\right)^2 - b\frac{\partial y}{\partial x} + c = 0.$$

Proof!!!

Characteristics (3/3)

This is quadratic equation for the slope of characteristic curve (dy/dx) having solution

$$\frac{dy}{dx} = \frac{b \pm \sqrt{b^2 - 4ac}}{2a}$$

Is the solution of quadratic equation correct? Check signs.

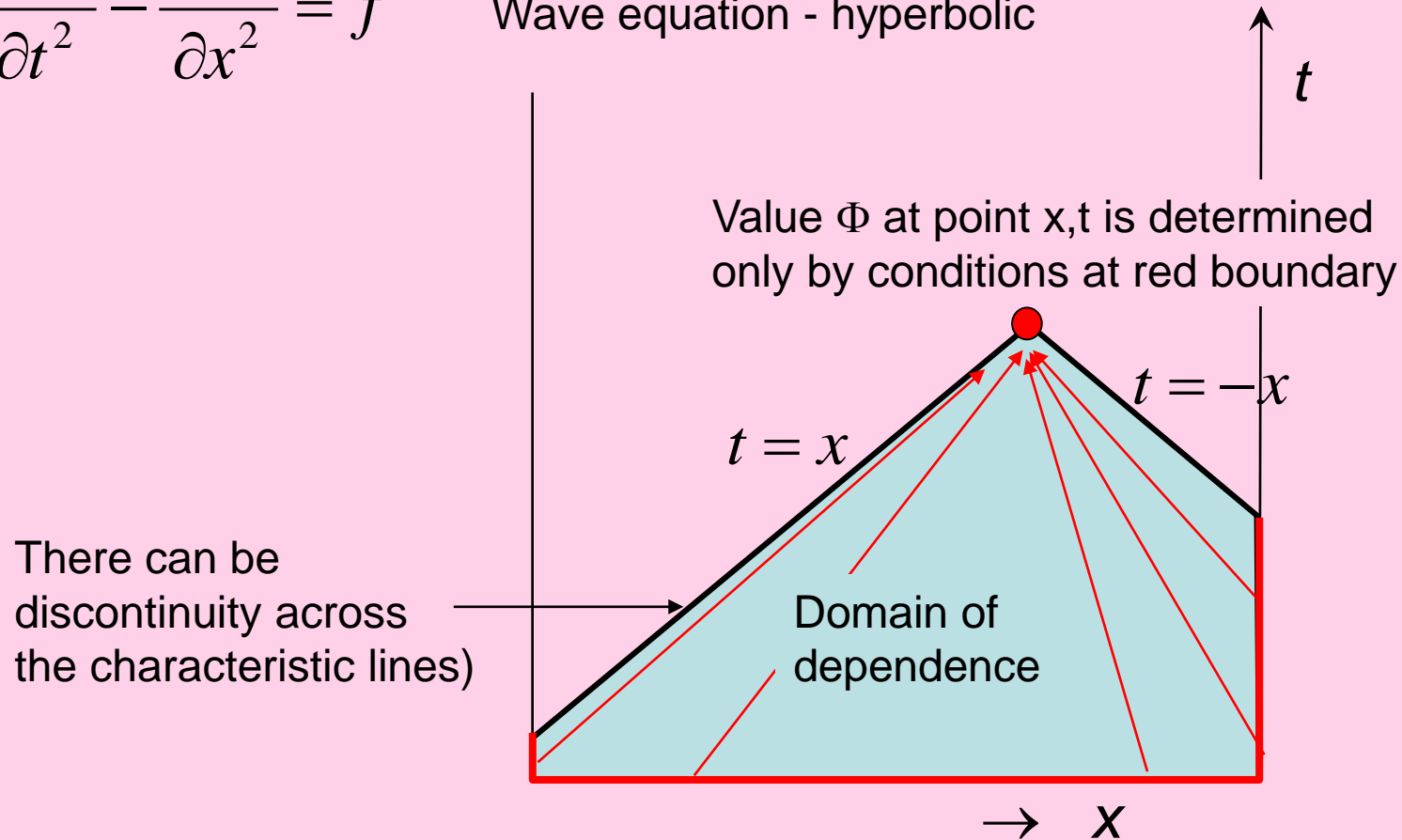
In the case that $b^2 - 4ac > 0$ there exist two real characteristics (hyperbolic equation), for $b^2 - 4ac = 0$ there is only one real characteristic (parabolic equation) and as soon as $b^2 - 4ac < 0$ there are no real characteristics (elliptic equation).

$\frac{\partial^2 \Phi}{\partial x^2} - \frac{\partial^2 \Phi}{\partial y^2} = f$	$a=1, b=0, c=-1$	$b^2 - 4ac = 4$	characteristics $\frac{dy}{dx} = \pm 1$
$\frac{\partial^2 \Phi}{\partial x^2} + \frac{\partial^2 \Phi}{\partial y^2} = f$	$a=1, b=0, c=1$	$b^2 - 4ac = -4$	characteristics $\frac{dy}{dx} = \pm i$ (not real)
$\frac{\partial^2 \Phi}{\partial x^2} - \frac{\partial \Phi}{\partial y} = f$	$a=1, b=0, c=0$	$b^2 - 4ac = 0$	characteristics $\frac{dy}{dx} = 0$

Characteristics

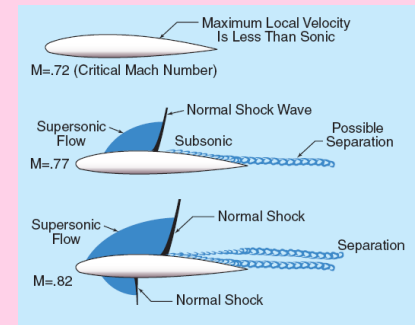
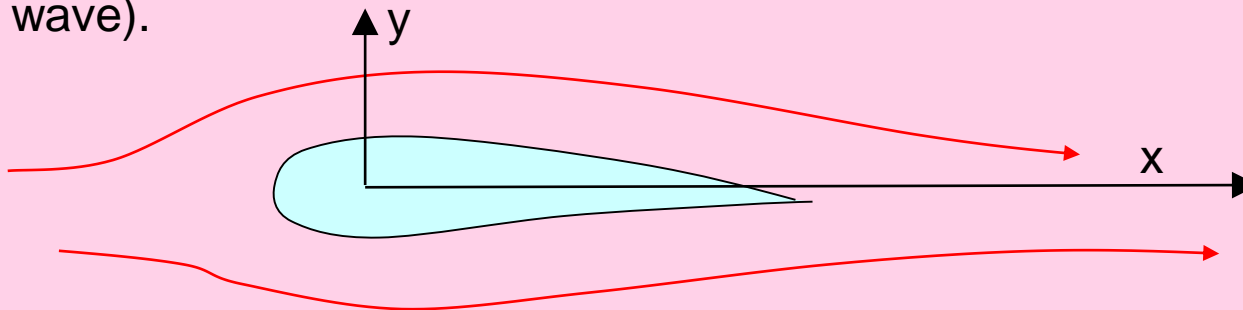
$$\frac{\partial^2 \Phi}{\partial t^2} - \frac{\partial^2 \Phi}{\partial x^2} = f$$

Wave equation - hyperbolic



PDE type - example

One and the same equation can be in some region elliptic, in other hyperbolic (for example regions of subsonic and supersonic flow, separated by a shock wave).



An example is [Prandl-Glauert equation](#) describing steady, inviscid, compressible and isentropic (adiabatic) flow of ideal fluid around a slender body (e.g. airfoil)

$$(1 - M^2) \frac{\partial^2 \Phi}{\partial x^2} + \frac{\partial^2 \Phi}{\partial y^2} = 0 \quad u = \frac{\partial \Phi}{\partial x}, \quad v = \frac{\partial \Phi}{\partial y}$$

Function $\Phi(x,y)$ is velocity potential, M is Mach number (ratio of velocity of fluid and speed of sound). For $M < 1$ (subsonic flow region) the equation is elliptic, for $M > 1$ (supersonic flow) the equation is hyperbolic. See [wikipedia](#).

Another example: [Laval nozzle](#)

PDE type – example PWV

Pulse Wave Velocity in elastic pipe
(latex tube, arteries)

Model-hyperbolic equations

Experiment-cross correlation technique
using high speed cameras

Macková, H. - Chlup, H. - Žitný, R.: Numerical model
for verification of constitutive laws of blood vessel
wall. Journal of Biomechanical Science and
Engineering. 2007, vol. 2, no. 2/1, p. s66.



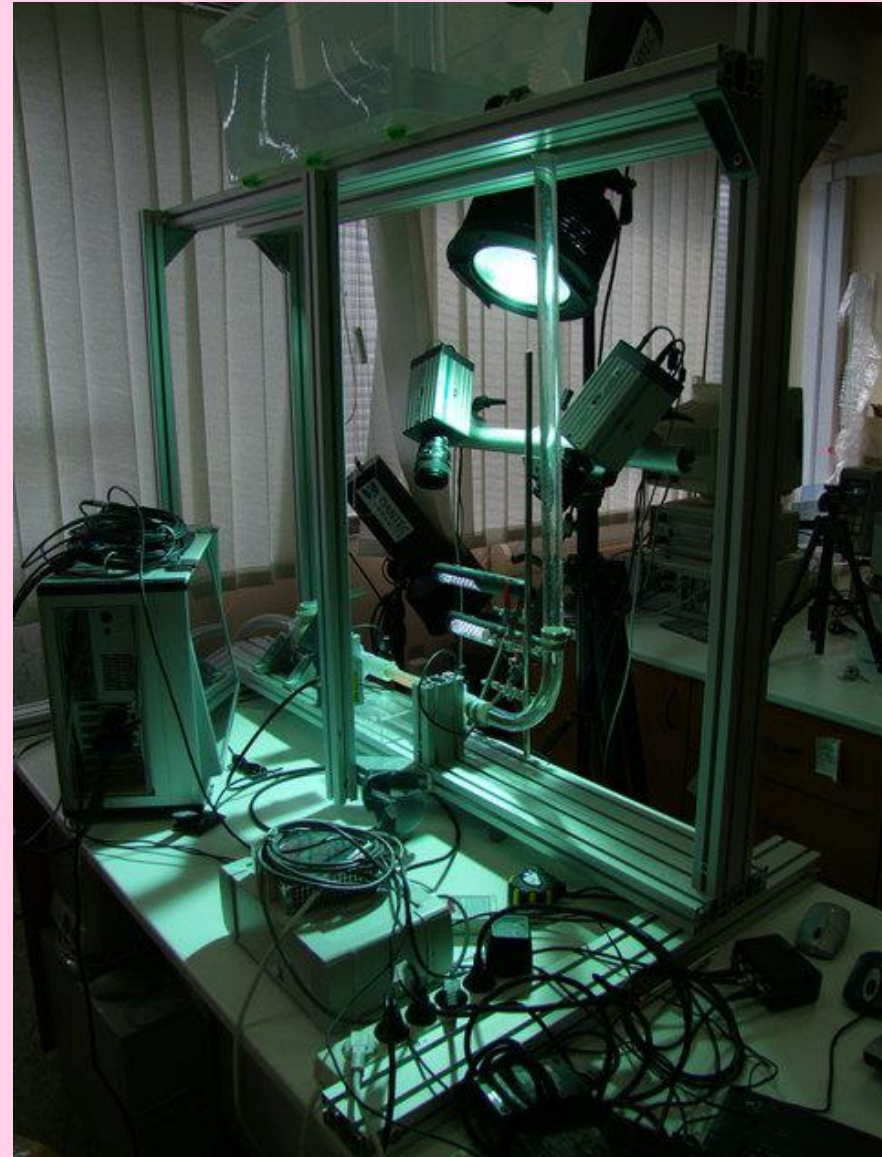
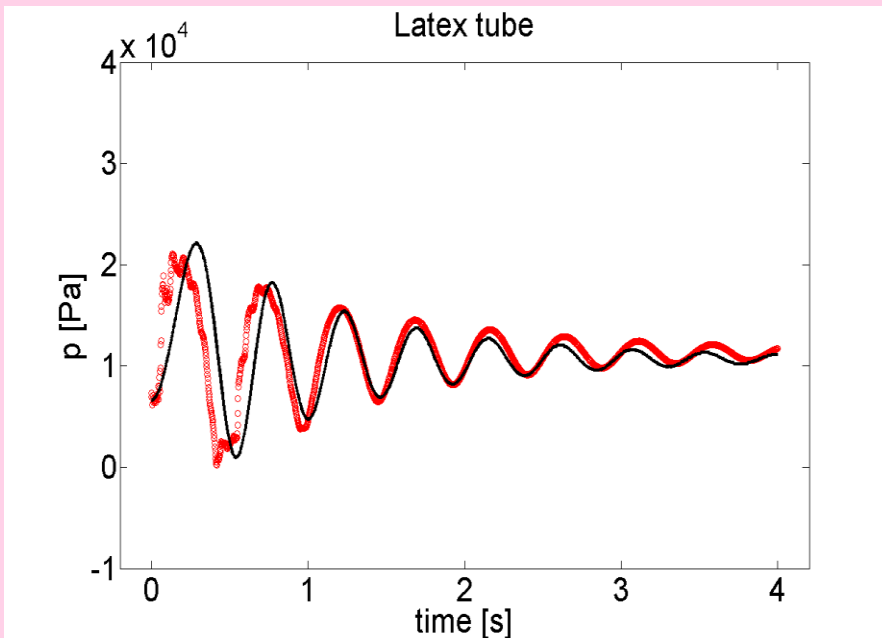
PDE type – example WH

Water Hammer experiment with elastic pipe (latex tube, artificial artery)

Model-hyperbolic equations

Experiment-cross correlation technique using high speed cameras

Pressure sensors



Hyperbolic equations WH

Flows in a pipe. Time dependent cross section $A(t,x)$, or time dependent mean velocity $v(t,x)$. Compressible fluid or elastic pipe. Relationship between volume and pressure is characterised by modulus of elasticity K [Pa]

$$\frac{\partial \rho}{\rho} = \frac{\partial p}{K}$$

related to speed of sound a $\frac{K}{\rho} = \frac{\partial p}{\partial \rho} = a^2$

Problem is to predict pressure and flowrate courses along the pipeline $p(t,x)$, $v(t,x)$. Basic equations: continuity and momentum balance (Bernoulli). In simplified form

$$\frac{\partial p}{\partial t} + K^* \frac{\partial v}{\partial x} = 0$$

$$K^* = \frac{K}{1 + \frac{K}{A} \frac{\partial A}{\partial p}}$$

$$\rho \frac{\partial v}{\partial t} + \frac{\partial p}{\partial x} + \frac{f \rho}{2D} v |v| = 0$$

neglected convective term. f -is friction factor

Velocity $v(t,x)$ can be eliminated by neglecting friction, giving

$$\frac{\partial^2 p}{\partial t^2} - a^2 \frac{\partial^2 p}{\partial x^2} = 0,$$

Speed of sound $a = \sqrt{\frac{K^*}{\rho}}$

How to derive equations of characteristics

$$\frac{\partial p}{\partial t} + \rho a^2 \frac{\partial v}{\partial x} = 0 \quad \text{multiply by } \lambda \text{ and add both equations}$$

$$\rho \frac{\partial v}{\partial t} + \frac{\partial p}{\partial x} = e_z$$

$$\lambda \left(\frac{\partial p}{\partial t} + \frac{1}{\lambda} \frac{\partial p}{\partial x} \right) + \rho \left(\frac{\partial v}{\partial t} + \lambda a^2 \frac{\partial v}{\partial x} \right) = e_z$$

this could be directional derivative
 this could be directional derivative

$$\frac{dp}{dt} = \frac{\partial p}{\partial t} + \frac{\partial x}{\partial t} \frac{\partial p}{\partial x} \quad \frac{dv}{dt} = \frac{\partial v}{\partial t} + \frac{\partial x}{\partial t} \frac{\partial v}{\partial x}$$

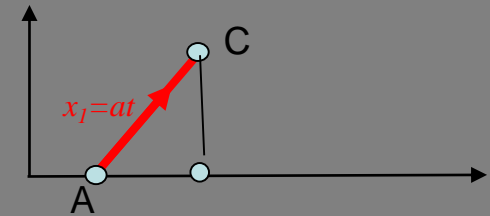
$$\frac{dx}{dt} = \frac{1}{\lambda} = \lambda a^2$$

$$\lambda = \pm \frac{1}{a}$$

$$\underbrace{\frac{dx}{dt}}_{\text{characteristic}} = a, \quad \underbrace{\frac{dx}{dt}}_{\text{characteristic}} = -a$$

There are two characteristic lines corresponding to two values of λ

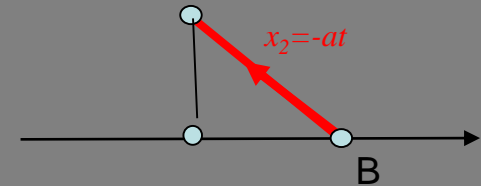
$$\lambda_1 = \frac{1}{a} \quad \frac{dx_1}{dt} = a \quad \frac{1}{a} \frac{dp}{dt} + \rho \frac{dv}{dt} = e_z$$



Integration along the characteristic line from A to C

$$\frac{1}{a} (p_c - p_A) + \rho (v_c - v_A) = -\Delta t \frac{f\rho}{2D} v_A |v_A|$$

$$\lambda_2 = -\frac{1}{a} \quad \frac{dx_2}{dt} = -a \quad \frac{-1}{a} \frac{dp}{dt} + \rho \frac{dv}{dt} = e_z$$



Integration along the characteristic line from B to C

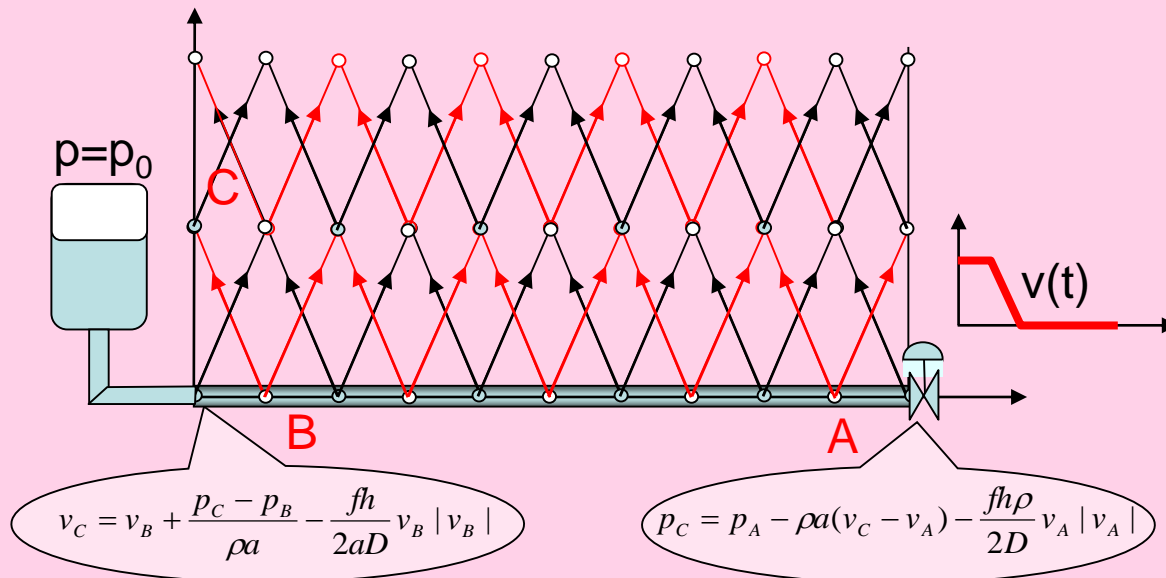
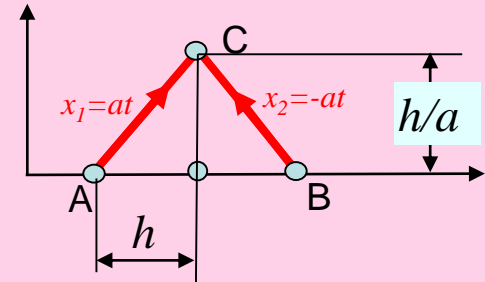
$$\frac{-1}{a} (p_c - p_B) + \rho (v_c - v_B) = -\Delta t \frac{f\rho}{2D} v_B |v_B|$$

Method of characteristic

Solution of previous system of 2 algebraic equations

$$v_C = \frac{1}{2} \left(\frac{p_A - p_B}{\rho a} + v_A + v_B - \frac{fh}{2aD} (v_A |v_A| + v_B |v_B|) \right)$$

$$p_C = \frac{a}{2} \left(\frac{p_A + p_B}{a} + \rho(v_A - v_B) + \frac{fh}{2aD} (v_B |v_B| - v_A |v_A|) \right)$$



Method of characteristic

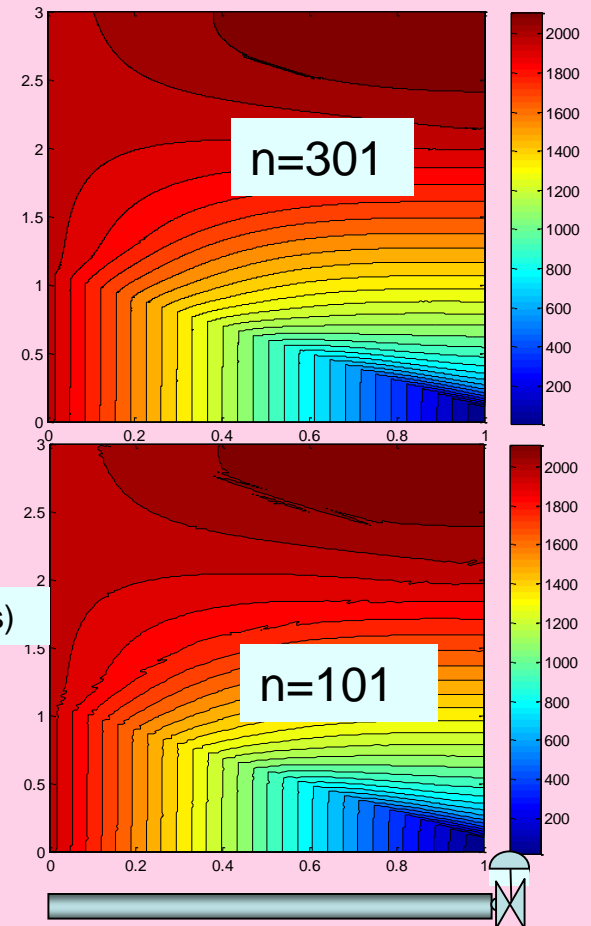
Pipe $L=1\text{m}$, $D=0.01\text{ m}$, speed of sound $a=1\text{ m/s}$, inlet pressure 2 kPa (steady velocity $v=0.6325\text{ m/s}$).

```

l=1;d=0.01;rho=1000;f=0.1;a=1;p0=2e3;
v0=(p0*2*d/(l*rho*f))^0.5
n=101;h=l/(n-1);v(1:n)=v0;p(1)=p0;
for i=2:n
    p(i)=p(i-1)-f*rho*v0^2*h/(2*d);
end
dt=h/a;tmax=3;itmax=tmax/dt;fhr=f*h/(2*a*d);
for it=1:itmax
    t=it*dt;
    for i=2:n-1
        pa=p(i-1);pb=p(i+1);va=v(i-1);vb=v(i+1);
        pc(i)=a/2*((pa+pb)/a+rho*(va-vb)+fhr*(vb*abs(vb)-va*abs(va)));
        vc(i)=0.5*((pa-pb)/(rho*a)+va+vb-fhr*(vb*abs(vb)+va*abs(va)));
    end
    pc(1)=p0; vb=v(2);pb=p(2);
    vc(1)=vb+(pc(1)-pb)/(a*rho)-fhr*vb*abs(vb);
    vc(n)=v0*valve(t); va=v(n-1);pa=p(n-1);
    pc(n)=pa-rho*a*(vc(n)-va)+f*h*rho/(2*d)*va*abs(va);
    vres(it,1:n)=vc(1:n); pres(it,1:n)=pc(1:n);
    p=pc;v=vc;
end
pmax=max(max(pres))/p0
x=linspace(0,1,n);
time=linspace(0,tmax,itmax);
contourf(x,time,pres,30)

```

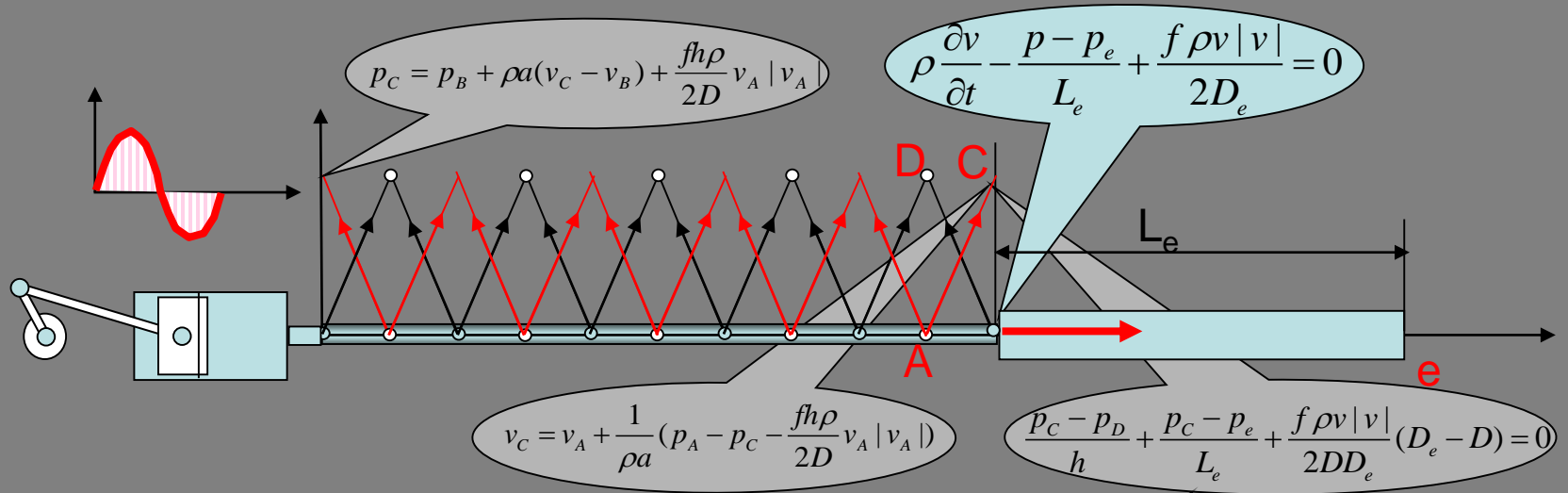
Pressure profiles



time (0-3 s)

Method of characteristic

Incorrect boundary condition at exit (elastic and rigid tube connection)



Bernoulli at an elastic tube

$$\rho \frac{\partial v}{\partial t} + \frac{\partial p}{\partial x} + \frac{f\rho v |v|}{2D} = 0$$

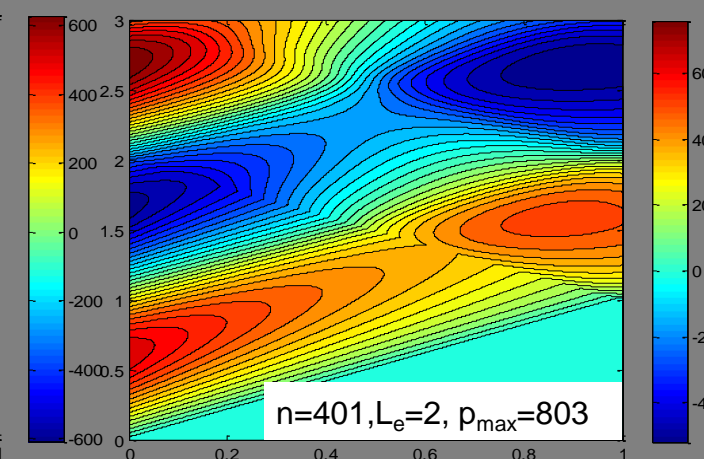
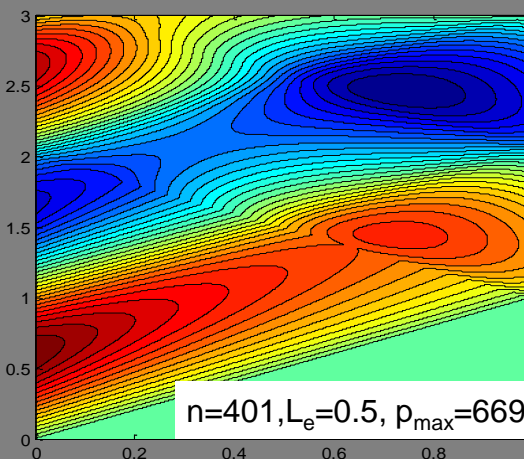
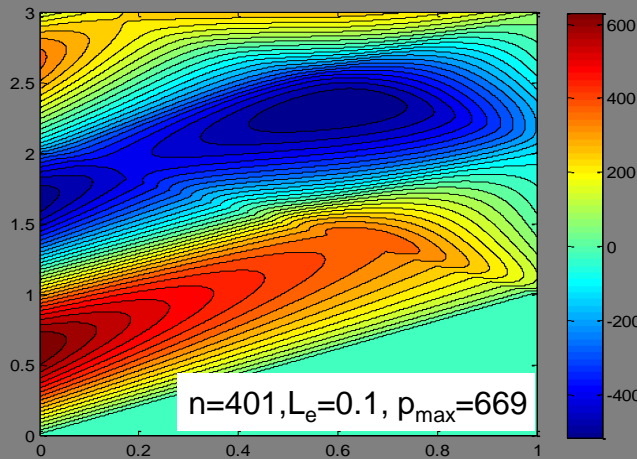
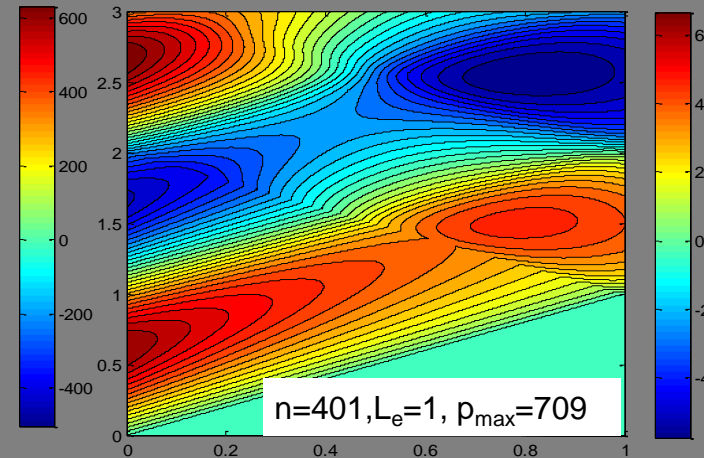
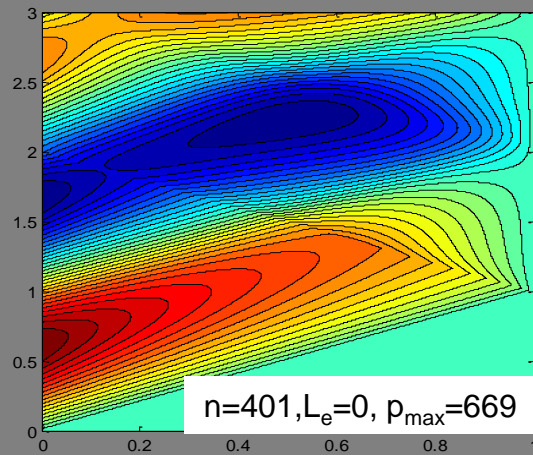
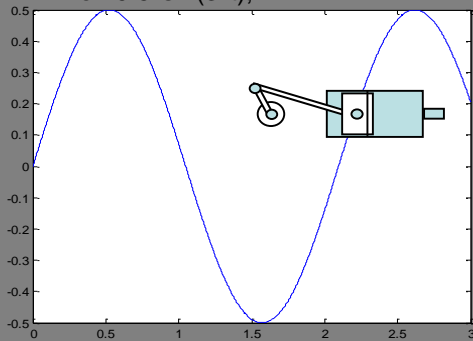
Bernoulli at a rigid tube

$$\frac{\partial p}{\partial x} + \frac{p - p_e}{L_e} + \frac{f\rho v |v|}{2DD_e} (D_e - D) = 0$$

Method of characteristic

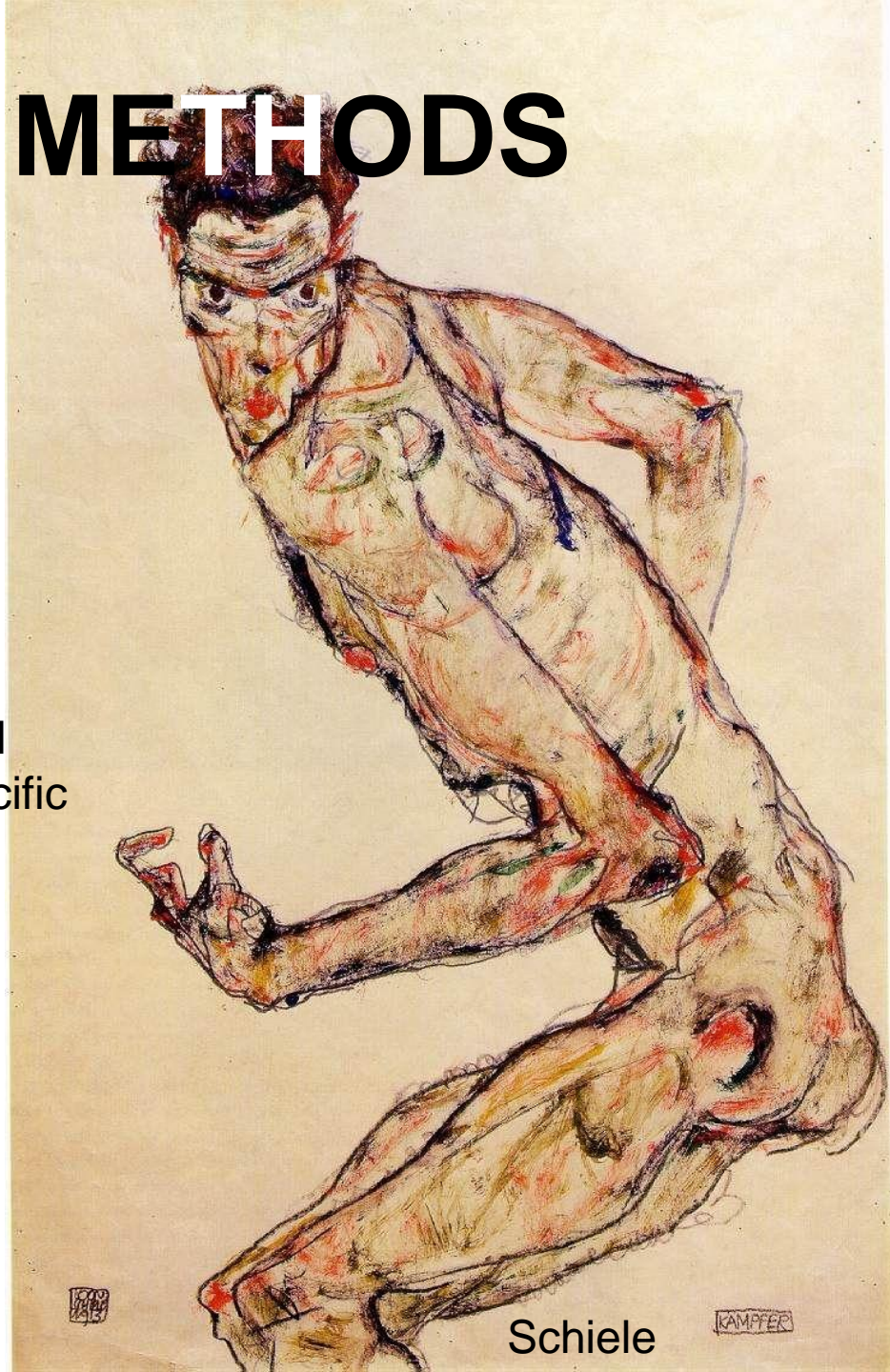
Classical numerical methods (Lax Wendroff), require at least slightly flexible connected pipe. MOC seems to be working with a rigid pipe too?

function vrel=pump(t)
vrel=0.5*sin(3*t);



NUMERICAL METHODS

The following slides are an attempt to overview frequently used numerical methods in CFD. It seems to me, that all these methods can be classified as specific cases of **Weighted Residual Methods**.



MWR methods of weighted residuals

Principles of **W**eighted **R**esidual **M**ethods will be demonstrated for a typical transport equation (steady state) – transport of matter, momentum or energy

The diagram shows the transport equation $\nabla \cdot (\vec{u}\Phi) - a\nabla^2\Phi + S = 0$ with three callout boxes pointing to its terms: 'Convective transport' points to $\nabla \cdot (\vec{u}\Phi)$, 'Dispersion (diffusion)' points to $a\nabla^2\Phi$, and 'Inner sources' points to S . The terms $\nabla \cdot (\vec{u}\Phi)$ and $a\nabla^2\Phi$ are circled in red in the original image.

$$\nabla \cdot (\vec{u}\Phi) - a\nabla^2\Phi + S = 0$$

Numerical solution $\Phi(x,y,z)$ is only an approximation and the previous equation will not be satisfied exactly, therefore the right hand side will be different from zero

$$\nabla \cdot (\vec{u}\Phi) - a\nabla^2\Phi + S = res(x, y, z)$$

$res(x,y,z)$ is a **RESIDUAL** of differential equation. A good approximation Φ should exhibit the smallest residuals as possible, or zero **weighted residuals**

$$\int_V res(x, y, z) \cdot w_i(x, y, z) dx dy dz = 0, \quad i = 1, 2, \dots, N$$

w_i are selected weighting functions, and V is the whole analyzed region.

Approximation – base

Approximation is selected as linear combination of BASE functions $N_j(x,y,z)$

$$\Phi(x, y, z) = \sum_j \Phi_j N_j(x, y, z)$$

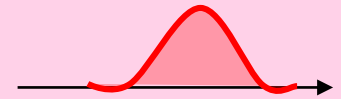
Substituting into weighted residuals we obtain system of algebraic equations for coefficients Φ_i (N-equations for N-selected weight functions w_i)

$$\begin{aligned} \int_V (\nabla \cdot (\vec{u}\Phi) - a\nabla^2\Phi + S) w_i dx dy dz &= \\ = \int_V (\nabla \cdot (\vec{u} \sum_j \Phi_j N_j) - a\nabla^2 \sum_j \Phi_j N_j + S) w_i dx dy dz &= 0 \end{aligned}$$

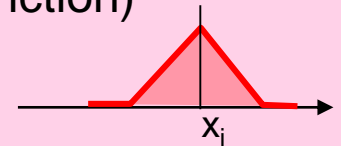
Weighting functions

Weighting functions can be suggested more or less arbitrarily in advance and independently of calculated solution. However there is always a systematic classification and families of weighting functions. Majority of numerical methods can be considered as MWR corresponding to different classes of weighting functions

- **Spectral methods** (analytical $w_i(x)$)
(Boundary element methods)



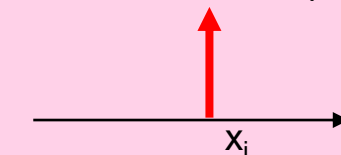
- **Finite element methods** (Galerkin – continuous weighting function)



- **Control volume methods** (discontinuous but finite weighting function)
(or Finite Volume methods) $w_i = h(x - x_{i-1/2}) - h(x - x_{i+1/2})$



- **Collocation methods** (zero residuals at nodal points, infinite delta functions)
(Finite Differences) $w_i = \delta(x - x_i)$



General characteristics

- Analytical approximation (analytical base functions)
- Very effective and fast (when using Fast Fourier Transform)
- Not very suitable for complex geometries (best case are rectangular regions)

$$T(x) = \sum_{j=0} T_j P_j(x)$$

SPECTRAL METHOD ORTHOGONAL POLYNOMIALS

Weight functions and base functions are selected as ORTHOGONAL functions (for example orthogonal polynomials) $P_j(x)$. Orthogonality in the interval x (a,b) means

$$\int_a^b g(x)P_i(x)P_j(x)dx = \delta_{ij}$$


In words: scalar product of different orthogonal functions is always zero.

Polynomial name	a	b	g(x)
Legendre	-1	1	1
Tschebyshev I	-1	1	$1/\sqrt{1-x^2}$
Tschebyshev II	-1	1	$\sqrt{1-x^2}$
Laguerre	0	∞	$\exp(-x)$
Hermite	$-\infty$	∞	$\exp(-x^2)$

WHY ORTHOGONAL?

Why not to use the simplest polynomials $1, x, x^2, x^3, \dots$? Anyway, orthogonal polynomials are nothing else than a linear combination of these terms? The reason is that for example the polynomials x^8 and x^9 look similar and are almost linearly dependent (it is difficult to see the difference by eyes if x^8 and x^9 are properly normalised). Weight functions and base functions should be as different (linearly independent) as possible. See different shapes of orthogonal polynomial on the next slide. Remark: May be you know, that linear polynomial regression fails for polynomials of degree 7 and higher. The reason are round-off errors and impossibility to resolve coefficients at higher order polynomial terms (using arithmetic with finite number of digits). You can perform linear regression with orthogonal polynomials of any degree without any problem.

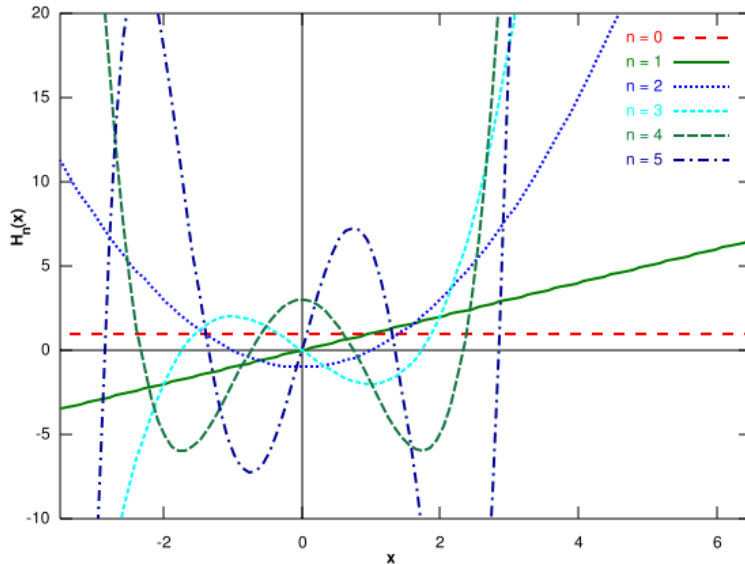
There is other reason. Given a function $T(x)$ it is quite easy to calculate coefficients of linear combination without necessity to solve a system of algebraic equations:

$$T(x) = \sum_{j=0} T_j P_j(x)$$

$$T_j = \int_a^b P_j(x) T(x) dx$$

Proof!!!

Orthogonal polynomials

HERMITE polynomial



$$H_0(x) = 1$$

$$H_1(x) = x$$

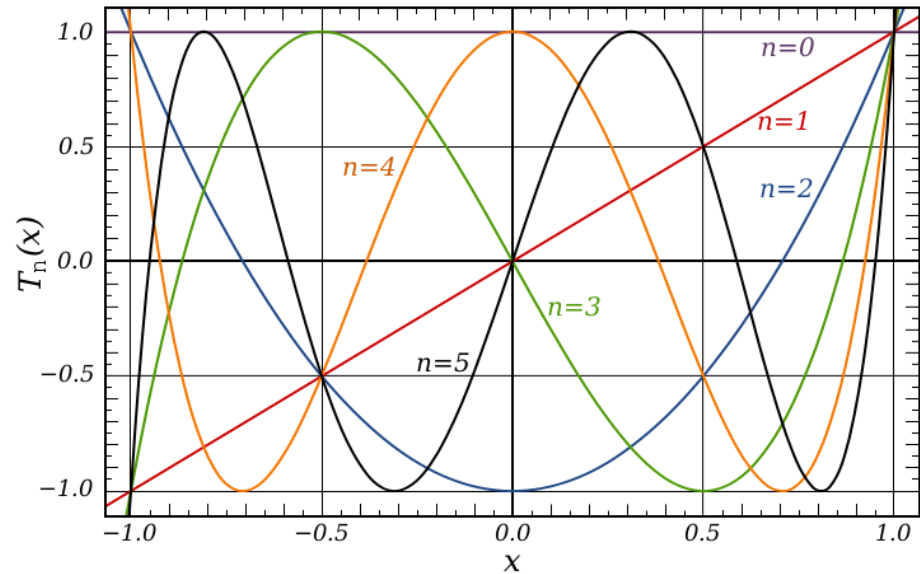
$$H_2(x) = x^2 - 1$$

$$H_3(x) = x^3 - 3x$$

$$H_4(x) = x^4 - 6x^2 + 3$$

$$H_5(x) = x^5 - 10x^3 + 15x$$

TSCHEBYSHEF I. polynomial



$$T_0(x) = 1$$

$$T_1(x) = x$$

$$T_2(x) = 2x^2 - 1$$

$$T_3(x) = 4x^3 - 3x$$

$$T_4(x) = 8x^4 - 8x^2 + 1$$

$$T_5(x) = 16x^5 - 20x^3 + 5x$$

Goniometric functions (sin, cos) are orthogonal in interval $(-\pi, \pi)$.

Orthogonality of. $P_n(x) = \cos nx$ follows from

$$\int_{-\pi}^{\pi} \cos mx \cos nxdx = \frac{1}{2} \int_{-\pi}^{\pi} (\cos(m-n)x + \cos(m+n)x) dx =$$

$$= \frac{1}{2} \left[\frac{\sin(m-n)x}{m-n} + \frac{\sin(m+n)x}{m+n} \right]_{-\pi}^{\pi} = \pi \quad \text{for } m=n, \text{ otherwise } 0$$

Proof!!!

In a similar way the orthogonality of $\sin nx$ can be derived. From the Euler's formula follows orthogonality of $P_j(x) = e^{ijx} = \cos jx + i \sin jx$

i-imaginary unit

Linear combination of $P_j(x)$ is called Fourier's expansion

$$T(x) = \sum_{j=0} T_j P_j(x)$$

The transformation $T(x)$ to T_j for $j=0, 1, 2, \dots$, is called Fourier transform and its discrete form is DFT $T(x_1), T(x_2), \dots, T(x_N)$ to T_1, T_2, \dots, T_N . DFT can be realized by FFT (Fast Fourier Transform) very effectively.

SPECTRAL METHOD EXAMPLE

Poisson's equation (elliptic). This equation describes for example temperature in solids with heat sources, Electric field, Velocity potential (inviscid flows).

$$\frac{\partial^2 T}{\partial y^2} + \frac{\partial^2 T}{\partial x^2} = f(x, y)$$

Fourier expansion of two variables x,y (i-imaginary unit, not an index)

$$T(x, y) = \sum T_{jk} e^{i(jx+ky)} \quad f(x, y) = \sum f_{jk} e^{i(jx+ky)}$$

Substituting into PDE $\sum -T_{jk} (j^2 + k^2) e^{i(jx+ky)} = \sum f_{jk} e^{i(jx+ky)}$

Evaluated Fourier
coefficients of solution

$$T_{jk} = -\frac{f_{jk}}{j^2 + k^2}$$

Technical realization

- Use FFT routine for calculation f_{jk}
- Evaluate T_{jk}
- $T(x,y)$ by inverse FFT

FINITE ELEMENT method

General characteristics

- Continuous (but not smooth) base as well as weighting functions
- Suitable for complicated geometries and structural problems
- Combination of fluid and structures (solid-fluid interaction)

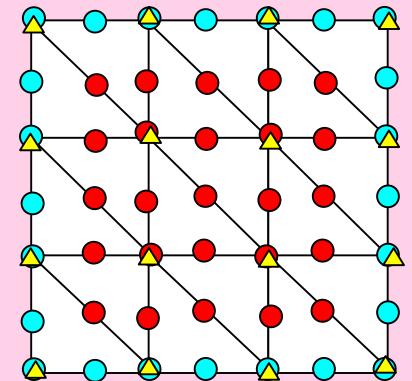
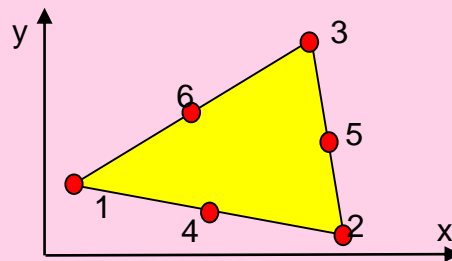
FINITE ELEMENT method

Base functions $N_i(x)$, $N_i(x,y)$ or $N_i(x,y,z)$ and corresponding weight functions are defined in each finite element (section, triangle, cube) separately as a polynomial (linear, quadratic,...). Continuity of base functions is assured by connectivity at nodes. Nodes x_j are usually at perimeter of elements and are shared by neighbours.

Base function N_i (identical with weight function w_i) is associated with node x_i and must fulfill the requirement: $N_i(x_j) = \delta_{ij}$ (base function is 1 in associated node, and 0 at all other nodes)

In CFD (2D flow) velocities are approximated by quadratic polynomial (6 coefficients, therefore 6 nodes ●) and pressures by linear polynomial (3 coefficients and nodes ▲). Blue nodes ● are prescribed at boundary.

Verify number of coeffs.!



FINITE ELEMENT example

Poisson's equation $\frac{\partial^2 T}{\partial y^2} + \frac{\partial^2 T}{\partial x^2} = f(x, y)$

Derive Green's theorem!

MWR and application of Green's theorem

$$\int_{\Omega} w \left(\frac{\partial^2 T}{\partial y^2} + \frac{\partial^2 T}{\partial x^2} - f(x, y) \right) d\Omega = - \int_{\Omega} \left(\frac{\partial w}{\partial x} \frac{\partial T}{\partial x} + \frac{\partial w}{\partial y} \frac{\partial T}{\partial y} + wf(x, y) \right) d\Omega = 0$$

Base functions are identical with weight function (Galerkin's method)

$$T(x) = \sum T_j N_j(x) \quad w_i(x) = N_i(x)$$

Resulting system of linear algebraic equations for T_i

$$\sum_{j=1}^n \int_{\Omega} \left(\frac{\partial N_i}{\partial x} \frac{\partial N_j}{\partial x} + \frac{\partial N_i}{\partial y} \frac{\partial N_j}{\partial y} \right) d\Omega T_j = \int_{\Omega} N_i f d\Omega$$

$$\sum_{j=1}^n A_{ij} T_j = \int_{\Omega} N_i f d\Omega$$

BOUNDARY element method

General characteristics

- Analytical (therefore continuous) weighting functions. Method evolved from method of singular integrals (BEM makes use analytical weight functions with singularities, so called fundamental solutions).
- Suitable for complicated geometries (potential flow around cars, airplanes...)
- Meshing must be done only at boundary. No problems with boundaries at infinity.
- Not so advantageous for nonlinear problem.

Introductory course on BEM including Fortran source codes is freely available in pdf ([Whye-Teong Ang](#) 2007)

BOUNDARY element example

Poisson's equation

$$\frac{\partial^2 T}{\partial y^2} + \frac{\partial^2 T}{\partial x^2} = f(x, y)$$

MWR and application of Green's theorem twice (second derivatives transferred to w)

$$-\iint_{\Omega} \left(\frac{\partial T}{\partial x} \frac{\partial w}{\partial x} + \frac{\partial T}{\partial y} \frac{\partial w}{\partial y} \right) dx dy + \int_{\Gamma} \left(n_x \frac{\partial T}{\partial x} + n_y \frac{\partial T}{\partial y} \right) w d\Gamma = \iint_{\Omega} f w dx dy$$

Green's theorem!

$$\iint_{\Omega} T \left(\frac{\partial^2 w}{\partial x^2} + \frac{\partial^2 w}{\partial y^2} \right) dx dy + \int_{\Gamma} \left(n_x \left(w \frac{\partial T}{\partial x} - T \frac{\partial w}{\partial x} \right) + n_y \left(w \frac{\partial T}{\partial y} - T \frac{\partial w}{\partial y} \right) \right) d\Gamma = \iint_{\Omega} f w dx dy$$

Weight functions are solved as a fundamental solution of adjointed equation

$$\frac{\partial^2 w_i}{\partial x^2} + \frac{\partial^2 w_i}{\partial y^2} = \delta(x - x_i, y - y_i)$$

Singularity: Delta function at a point x_i, y_i

Delta function!

Solution (called Green's function) is

$$w_i(x, y) = \frac{1}{2\pi} \ln \frac{1}{r_i}$$

$$r_i = \sqrt{(x - x_i)^2 + (y - y_i)^2}$$

Verify!

BOUNDARY element example

$$\iint_{\Omega} T \left(\frac{\partial^2 w}{\partial x^2} + \frac{\partial^2 w}{\partial y^2} \right) dx dy + \int_{\Gamma} \left(n_x \left(w \frac{\partial T}{\partial x} - T \frac{\partial w}{\partial x} \right) + n_y \left(w \frac{\partial T}{\partial y} - T \frac{\partial w}{\partial y} \right) \right) d\Gamma = \iint_{\Omega} f w dx dy$$

Substituting $w=w_i$ (Green's function at point i)

$$T(x_i, y_i) = - \int_{\Gamma} \left[w_i \left(n_x \frac{\partial T}{\partial x} + n_y \frac{\partial T}{\partial y} \right) - T \left(n_x \frac{\partial w_i}{\partial x} + n_y \frac{\partial w_i}{\partial y} \right) \right] d\Gamma + \iint_{\Omega} f w_i dx dy$$

Solution T at arbitrary point x_i, y_i is expressed in terms of boundary values

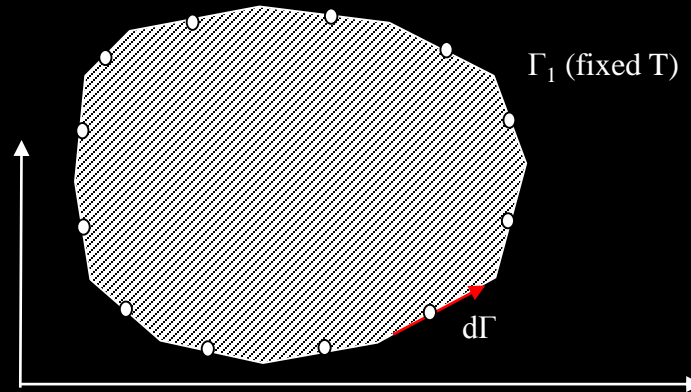
$$T(\Gamma) = \sum_{j=1}^N T_j N_j(\Gamma)$$

$$\frac{\partial T}{\partial n}(\Gamma) = \sum_{j=1}^N T_{nj} N_j(\Gamma)$$

At any boundary point must be specified either T or normal derivative of T , not both simultaneously.

Γ_2 (normal derivative)

Γ_1 (fixed T)

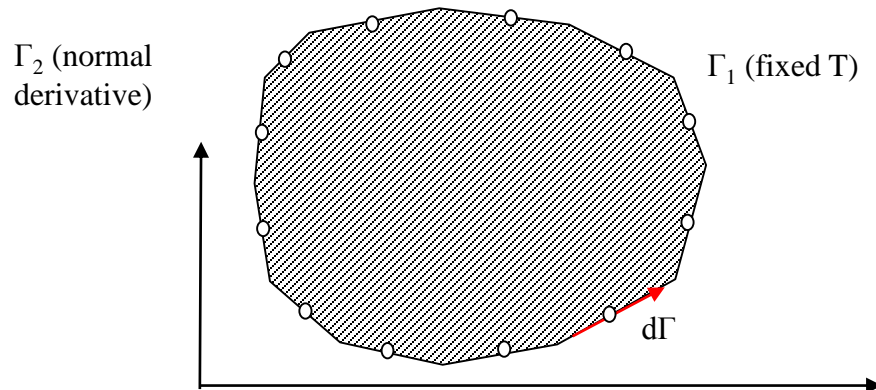


BOUNDARY element example

Values at boundary nodes not specified as boundary conditions must be evaluated from the following system of algebraic equations

$$0 = - \int_{\Gamma} [T_{nj} w_i - T_j (n_x \frac{\partial w_i}{\partial x} + n_y \frac{\partial w_i}{\partial y})] N_j d\Gamma + \iint_{\Omega} f w_i dx dy$$

$$T_{nj} \int_{\Gamma} w_i N_j d\Gamma + T_j \int_{\Gamma} (n_x \frac{\partial w_i}{\partial x} + n_y \frac{\partial w_i}{\partial y}) N_j d\Gamma = \iint_{\Omega} f w_i dx dy$$



FINITE VOLUME method

General characteristic:

- Discontinuous weight functions
- Structured, unstructured meshes.
- Conservation of mass, momentum, energy (unlike FEM).
- Only one value is assigned to each cell (velocities, pressures).

Will be discussed in more details in this course

FINITE VOLUME example

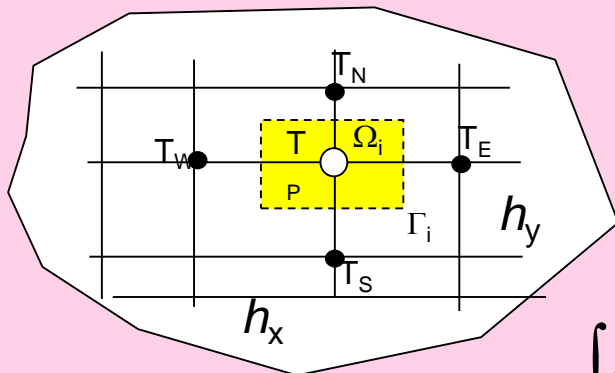
Poisson's equation $\frac{\partial^2 T}{\partial y^2} + \frac{\partial^2 T}{\partial x^2} = f(x, y)$

MWR (Green's theorem cannot be applied because $w(x)$ is discontinuous)

$$\int_{\Omega} w \left(\frac{\partial^2 T}{\partial y^2} + \frac{\partial^2 T}{\partial x^2} - f(x, y) \right) d\Omega = \int_{\Omega_i} \left(\frac{\partial^2 T}{\partial y^2} + \frac{\partial^2 T}{\partial x^2} - f(x, y) \right) d\Omega = \int_{\Omega_i} (\nabla \cdot \nabla T - f(x, y)) d\Omega = 0$$

Gauss theorem (instead of Green's)

$$\int_{\Omega_i} (\nabla \cdot \nabla T - f(x, y)) d\Omega = \int_{\Gamma_i} \vec{n} \cdot \nabla T d\Gamma - \int_{\Omega_i} f(x, y) d\Omega = 0$$



$$\int_{\Omega_i} f(x, y) d\Omega \cong f(x_P, y_P) h_x h_y$$

$$\int_{\Gamma_i} \vec{n} \cdot \nabla T d\Gamma \cong \frac{T_E - T_P}{x_E - x_P} h_y + \frac{T_N - T_P}{y_N - y_P} h_x + \frac{T_W - T_P}{x_W - x_P} h_y + \frac{T_S - T_P}{y_S - y_P} h_x$$

CFD2 FINITE DIFFERENCES method

General characteristic:

- Substitution derivatives in PDE by finite differences.
- Transformation from computational (rectangular) to physical (curvilinear) domain

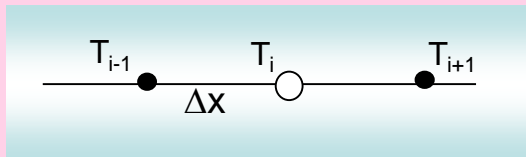
Suitable first of all for gas dynamic (compressible flows – aerodynamics)

Will be discussed in more details in this course

FINITE DIFFERENCES

Finite differences methods specify zero residuals in selected nodes (the same requirement as in classical collocation method). However, residuals in nodes are not calculated from a global analytical approximation (e.g. from orthogonal polynomials), but from local approximations in the vicinity of zero residual node.

It is very easy technically: Each **derivative** in PDE is substituted by finite **difference** evaluated from neighbouring nodal values.



$$\frac{\partial T}{\partial x} \cong \frac{T_i - T_{i-1}}{\Delta x} \quad \text{Upwind 1st order}$$

$$\frac{\partial T}{\partial x} \cong \frac{T_{i+1} - T_{i-1}}{2\Delta x} \quad \text{Central differencing 2st order}$$

$$\frac{\partial^2 T}{\partial x^2} \cong \frac{T_{i-1} - 2T_i + T_{i+1}}{\Delta x^2} \quad \text{Central differencing 2st order}$$

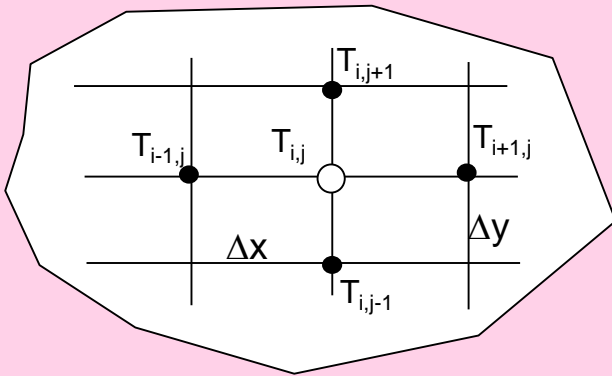
Verify!

FINITE DIFFERENCES example

Poisson's equation

$$\frac{\partial^2 T}{\partial x^2} + \frac{\partial^2 T}{\partial y^2} = f(x, y)$$

$$\frac{T_{i-1,j} - 2T_{i,j} + T_{i+1,j}}{\Delta x^2} + \frac{T_{i,j-1} - 2T_{i,j} + T_{i,j+1}}{\Delta y^2} = f_{i,j}$$



Elliptic equation – it is necessary to solve a large system of algebraic equations

FINITE DIFFERENCES example

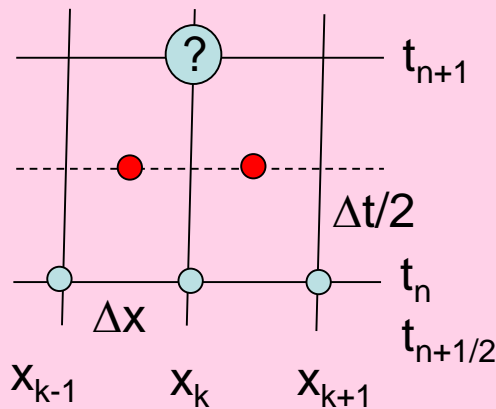
Wave equation (pure convection)

Hyperbolic PDE-it is possible to use explicit method

$$\frac{\partial T}{\partial t} + c \frac{\partial T}{\partial x} = 0$$

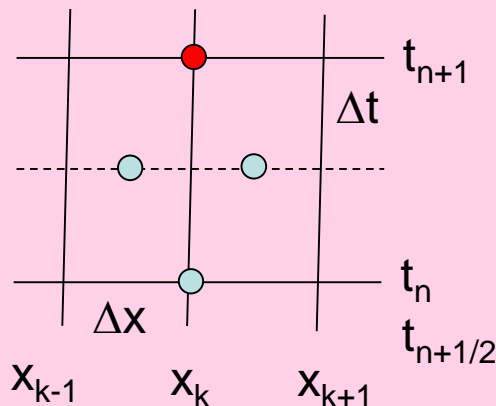
exact solution
 $T(t, x) = T(x - ct)$

Lax Wendroff method



First step – Lax's scheme with time step $\Delta t/2$

$$\frac{T_{k-1/2}^{n+1/2} - \frac{T_{k-1}^n + T_k^n}{2}}{\Delta t/2} + c \frac{T_k^n - T_{k-1}^n}{\Delta x} = 0 \quad \frac{T_{k+1/2}^{n+1/2} - \frac{T_k^n + T_{k+1}^n}{2}}{\Delta t/2} + c \frac{T_{k+1}^n - T_k^n}{\Delta x} = 0$$



Second step – central differences

$$\frac{T_k^{n+1} - T_k^n}{\Delta t} + c \frac{T_{k+1/2}^{n+1/2} - T_{k-1/2}^{n+1/2}}{\Delta x} = 0$$

FINITE DIFFERENCES example

Wave equation (pure convection)

Stability restriction when using explicit methods

$$CFL = \frac{c\Delta t}{\Delta x} < 1$$

```
dt=0.011;c=1;l=1;n=101;dx=l/(n-1);cfl=c*dt/dx
```

```
for i=1:n
```

```
  x(i)=(i-1)*dx;
```

```
  if x(i)<0.1
```

```
    t0(i)=0;
```

```
  else
```

```
    t0(i)=1;
```

```
  end
```

```
end
```

```
tmax=1.;itm=tmax/dt;
```

```
for it=1:itm
```

```
  for i=2:n-1
```

```
    ta(i)=(t0(i-1)+t0(i))/2-cfl*(t0(i)-t0(i-1))/2;
```

```
  end
```

```
  ta(1)=t0(1);ta(n)=t0(n);
```

```
  for i=2:n-1
```

```
    t(i)=t0(i)-cfl*(ta(i+1)-ta(i));
```

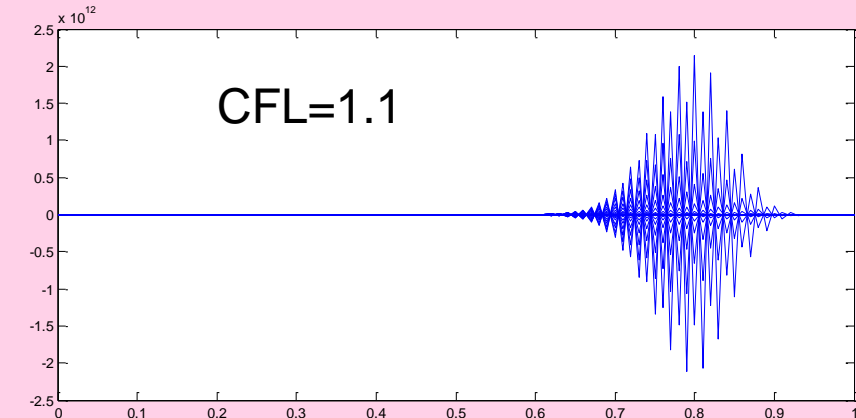
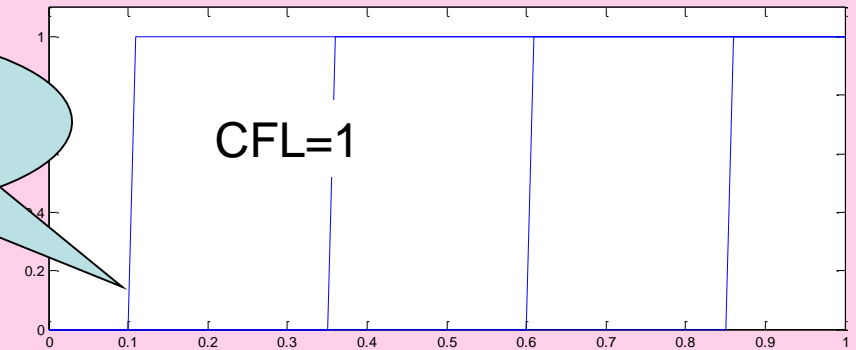
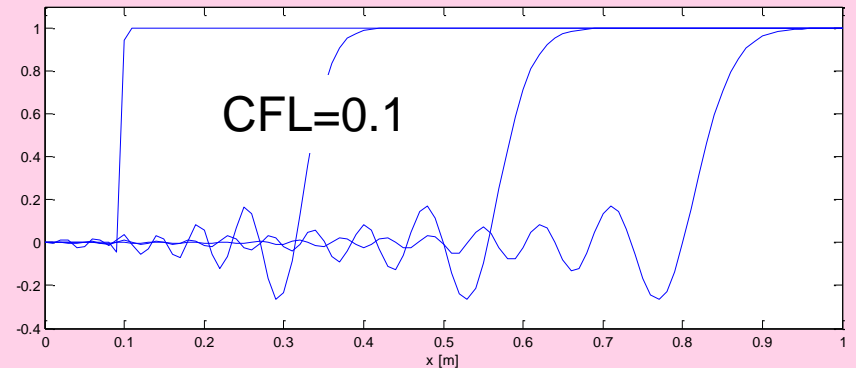
```
  end
```

```
  t(1)=t0(1);t(n)=t0(n);
```

```
  tres(it,:)=t(:); t0=t;
```

```
end
```

in this case the PDE is integrated along characteristic



MESHLESS methods

General characteristics

- Not available in commercial software packages
- Suitable for problems with free boundary
- Multiphase problems
- Easy remeshing (change of geometry) / in fact no meshing is necessary

MESHLESS methods

There exist many methods that can be classified as meshless, for example [SPH](#) (smoothed particle hydrodynamics), [Lattice Boltzman](#) (model of particles), [RKP](#) (Reproducing Kernel Particle method, Liu: [large deformation Mooney](#)), [MLPG](#) (Meshless Local Petrov Galerkin), [RBF](#) (Radial basis function, [wave equation](#)). All the methods approximate solution by the convolution integrals

$$\Phi^h(\vec{x}) = \int_{\Omega} \underbrace{c(\vec{x}, \vec{y})}_{\substack{\text{correction applied} \\ \text{at MLS, RKP methods}}} \underbrace{w(\vec{x} - \vec{y}, h)\Phi(\vec{y})}_{\text{classical SPH-convolution}} d\vec{y}$$

Recommended literature: Shaofan Li, Wing Kam Liu: Meshfree Particle Method, Springer Berlin 2007 (MONOGRAPHy analyzing most of the mentioned method and applications in mechanics of elastoplastic materials, transient phenomena, fracture mechanics, fluid flowm biological systems, for example red blood cell flow, heart valve dynamics). Summary of Galerkin Petrov integral methods Atluri S.N., Shen S.: The meshless local Petrov Galerkin (MLPG) method, CMES, vol.3, No.1, (2002), pp.11-51. Collocaton method: Shu C., Ding H., Yeo K.S.: Local radial basis function-based differential quadrature method and its application to solve two dimensional incompressible Navier Stokes equations, Comp.Methods Appl.Mech.Engng, 192 (2003), pp.941-954

CFD2 MESHLESS methods collocation

Radial base functions $N_j(x) = \varphi(r_j)$

where $r_j = \|x - x_j\|$ is simply a distance from node j .

Most frequently used radial base functions

linear

$$\varphi(r) = r$$

cubic

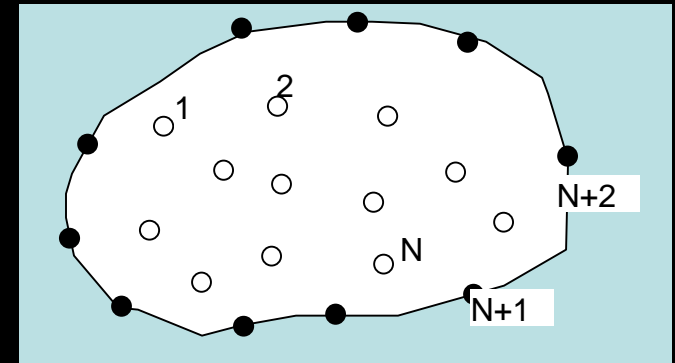
$$\varphi(r) = r^3$$

Gaussian

$$\varphi(r) = e^{-cr^2}$$

multiquadrics

$$\varphi(r) = \sqrt{r^2 + c^2}$$



MESHLESS methods EXAMPLE

Poisson's equation $\frac{\partial^2 T}{\partial y^2} + \frac{\partial^2 T}{\partial x^2} = f(x, y)$

Boundary conditions $T = g(x, y)$

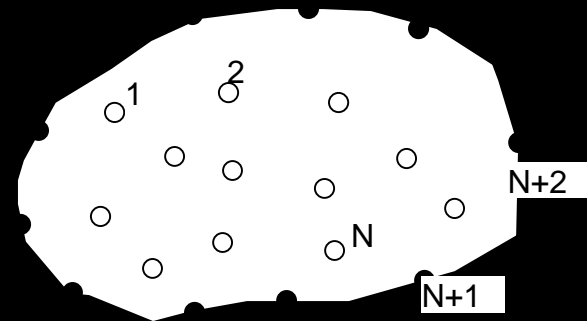
Approximation $T(x, y) = \sum_{j=1}^n T_j \varphi(r_j)$ $r_j = \sqrt{(x - x_j)^2 + (y - y_j)^2}$

$i=1, 2, \dots, N$
(inner points)

$$\sum_{j=1}^n \left(\frac{\partial^2 \varphi(r_j)}{\partial x^2} + \frac{\partial^2 \varphi(r_j)}{\partial y^2} \right) T_j = f(x_i, y_i)$$

$i=N+1, N+2, \dots, n$
(boundary)

$$\sum_{j=1}^n T_j \varphi(r_j) = g(x_i, y_i)$$



For multiquadric radial function

$$\varphi(r_j) = \sqrt{r_j^2 + c^2} = \sqrt{(x - x_j)^2 + (y - y_j)^2 + c^2}$$

$$\frac{\partial^2 \varphi}{\partial x^2} = \frac{(y - y_j)^2 + c^2}{\sqrt{r_j^2 + c^2}}$$

$$\frac{\partial^2 \varphi}{\partial y^2} = \frac{(x - x_j)^2 + c^2}{\sqrt{r_j^2 + c^2}}$$

MESHLESS method EXAMPLE RBF

Result is a system of n-linear algebraic equations that can be solved by any solver. In case of more complicated and nonlinear equations (Navier Stokes equations) the system can be solved for example by the least square optimization method, e.g. Marquardt Levenberg.

Few examples of papers available from Science Direct

Applied Mathematical Modelling 32 (2008) 1848–1858

Direct solution of Navier–Stokes equations by radial basis functions

G. Demirkaya ^a, C. Wafo Soh ^b, O.J. Ilegbusi ^{a,*}

Abstract

The pressure–velocity formulation of the Navier–Stokes (N–S) equation is solved using the radial basis functions (RBF) collocation method. The non-linear collocated equations are solved using the Levenberg–Marquardt method. The primary novelty of this approach is that the N–S equation is solved directly, instead of using an iterative algorithm for the primitive variables. Two flow situations are considered: Couette flow with and without pressure gradient, and 2D laminar flow in a duct with and without flow obstruction. The approach is validated by comparing the Couette flow results with the analytical solution and the 2D results with those obtained using the well-validated CFD-ACE™ commercial package.

© 2007 Published by Elsevier Inc.

Keywords: Meshless method; Radial basis functions; Navier–Stokes equations

2.2. Governing equation

In this section, the new RBF method is described. It is then used to predict the velocity and pressure distribution in a two-dimensional channel flow. The flow is assumed to be steady, viscous and incompressible. The Navier–Stokes equations for the flow in Cartesian coordinates are

$$\frac{\partial u^*}{\partial x^*} + \frac{\partial v^*}{\partial y^*} = 0, \quad (1)$$

$$u^* \frac{\partial u^*}{\partial x^*} + v^* \frac{\partial u^*}{\partial y^*} = -\frac{\partial p^*}{\partial x^*} + \frac{1}{Re} \left(\frac{\partial^2 u^*}{\partial x^{*2}} + \frac{\partial^2 u^*}{\partial y^{*2}} \right), \quad (2)$$

$$u^* \frac{\partial v^*}{\partial x^*} + v^* \frac{\partial v^*}{\partial y^*} = -\frac{\partial p^*}{\partial y^*} + \frac{1}{Re} \left(\frac{\partial^2 v^*}{\partial x^{*2}} + \frac{\partial^2 v^*}{\partial y^{*2}} \right) \quad (3)$$

in which all variables are non-dimensionalized, u^* and v^* represent the velocity components in the Cartesian coordinate directions x^* and y^* , respectively, p^* is the pressure, and Re is the Reynolds number ($\rho U_\infty D / \mu_\infty$) where D is the characteristic length of the domain, and ρ_∞ and U_∞ are the reference density and mean velocity, respectively. The Cartesian coordinates x^* and y^* are non-dimensionalized with respect to D , u^* and v^* are non-dimensionalized with respect to U_∞ , and finally, p^* is non-dimensionalized with respect to the dynamic pressure $\rho_\infty U_\infty^2$.

MESHLESS method EXAMPLE RBF

2.3.2. Radial basis function (RBF)

Consider the problem of finding a function whose values are known at a finite number of locations N . We may solve this problem by assuming that the unknown function is a linear combination of a complete set of N functions. The coefficients of the linear combination are obtained by solving a linear system resulting from forcing the linear combination to take the given values at the N locations. In the RBF approach the complete set of N functions are translated radial functions. Specifically, the approximation of a function $f(x)$, using RBF is

$$f(x) \cong \sum_{j=1}^N \alpha_j \Psi(\|x - x_j\|), \tag{4}$$

where $\| \ \|$ is the Euclidian norm, N is the number of total collocation points, α_j 's are the unknown coefficients to be determined and Ψ is the radial basis function. The interpolation coefficients $\alpha_1, \alpha_2, \dots, \alpha_N$ are determined by solving the linear system of equations:

$$f(x_i) \cong \sum_{j=1}^N \alpha_j \Psi(r_{ij}), \quad i = 1, \dots, N, \tag{5}$$

where $r_{ij} = \sqrt{(x_i - x_j)^2}$. The system of Eq. (5) can be written as

$$\underbrace{\begin{pmatrix} \Psi(0) & \Psi(r_{12}) & \Psi(r_{13}) & \cdots & \Psi(r_{1N}) \\ \Psi(r_{21}) & \Psi(0) & \Psi(r_{23}) & \cdots & \Psi(r_{2N}) \\ \vdots & \vdots & \vdots & & \vdots \\ \Psi(r_{N1}) & \Psi(r_{N2}) & \Psi(r_{N3}) & \cdots & \Psi(r_{NN}) \end{pmatrix}}_A \underbrace{\begin{pmatrix} \alpha_1 \\ \alpha_2 \\ \vdots \\ \alpha_N \end{pmatrix}}_\alpha = \underbrace{\begin{pmatrix} f_1 \\ f_2 \\ \vdots \\ f_N \end{pmatrix}}_{f_i} \tag{6}$$

- (a) Multi-quadratics (MQs): $\Psi(r) = \sqrt{r^2 + c^2}, c > 0$.
- (b) Thin-plate splines (TPS): $\Psi(r) = r^{2n} \log(r), n$ is an integer.
- (c) Gaussians: $\Psi(r) = e^{-cr^2}, c > 0$.
- (d) Inverse MQs: $\Psi(r) = \frac{1}{\sqrt{r^2 + c^2}}, c > 0$.

This radial base function (TPS) was used in this paper

MESHLESS method EXAMPLE RBF

2.4. Expansion of the Navier–Stokes and boundary conditions by RBF

The velocity and pressure terms are globally expanded by collocation of all the points on the boundary and domain as

$$u_i = \sum_{a=1}^{NB+NI} \alpha_{ia} \Psi(\|\vec{r} - \vec{r}_a\|) \quad i = 1, 2 \quad (u^* = u_1 \quad \text{and} \quad v^* = u_2), \quad (8)$$

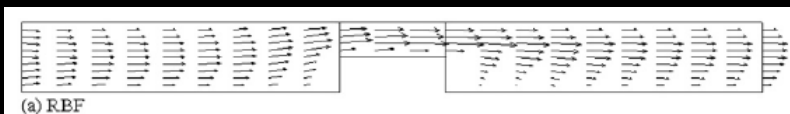
$$p^* = \sum_{a=1}^{NB+NI} \alpha_{0a} \Psi(\|\vec{r} - \vec{r}_a\|), \quad (9)$$

where NB is the total number of boundary points enclosed in the domain, NI is the total internal points in the domain, α_i are the expansion coefficients and Ψ is the radial basis expansion function.

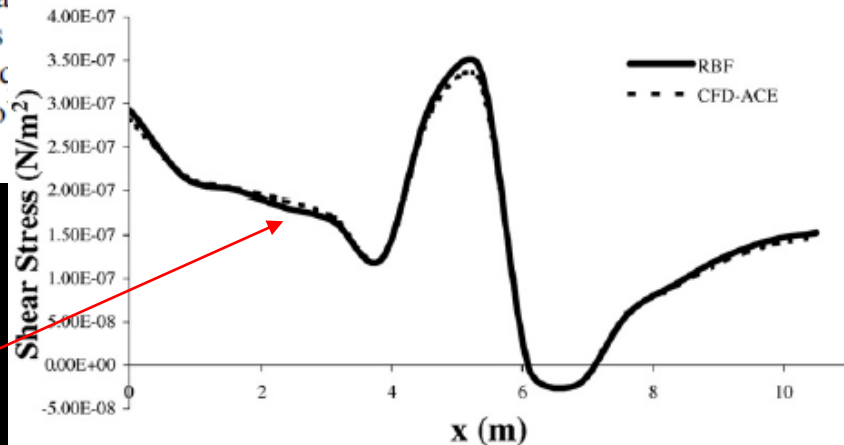
The Navier–Stokes and boundary condition equations together constitute a system of non-linear equations, which are to be solved. The expanded velocity and pressure terms and their first and second derivatives are directly inserted into the equations. The boundary condition equations are collocated at the boundary points ($i = 1..NB$) and the continuity and momentum equations are collocated at the interior domain points ($i = NB + 1..NB + NI$). Then a non-linear system of equations for the unknown expansion coefficient α is formed as

$$F(\alpha) = 0.$$

This non-linear system can be solved by the least-square optimization method [30–32]. The Levenberg–Marquardt algorithm is a sum of a multivariate function that is expressed as the sum of squares. It has become a standard technique for non-linear least-squares problems [30–32] for further details of this method.



Shear Stress along the lower wall



Comparison with results obtained by FVM package CFD-ACE



ELSEVIER

Contents lists available at ScienceDirect

Engineering Analysis with Boundary Elements

journal homepage: www.elsevier.com/locate/enganabound

A localized collocation meshless method (LCMM) for incompressible flows CFD modeling with applications to transient hemodynamics

Z. El Zahab^a, E. Divo^b, A.J. Kassab^{a,*}^a Department of Mechanical, Materials and Aerospace Engineering, University of Central Florida, USA^b Engineering Technology Department, University of Central Florida, P.O. Box 162450, Orlando, FL 32816-2450, USA

ARTICLE INFO

Article history:

Received 30 October 2008

Accepted 18 March 2009

Available online 15 May 2009

Keywords:

Meshless methods

CFD

Upwinding

Limiters

Incompressible flows

ABSTRACT

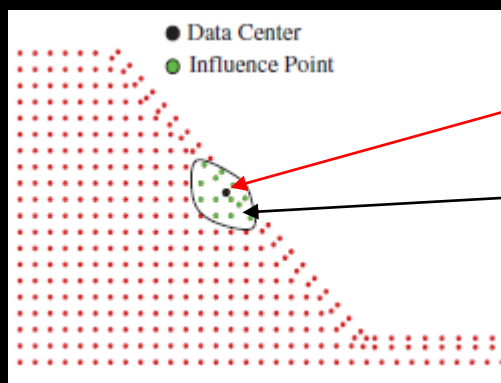
The current paper reports on the development and validation of a localized collocation meshless method (LCMM) to model laminar incompressible flows. A high order upwinding scheme was devised to dampen the numerical oscillations arising in convection-dominated flows. Subsequently, the LCMM was analytically validated and demonstrated to yield third-order accurate solutions when compared to a benchmark analytical decaying vortex solution. Numerical validations are provided by comparison with the finite volume commercial (FVM) solver Fluent 6.2. The flow geometry for the numerical validation arises from a biomedical application that consists of modeling blood flow in the interconnection between a bypass graft and an artery. Very good agreement was found between the LCMM and the FVM.

© 2009 Elsevier Ltd. All rights reserved.

MESHLESS method EXAMPLE RBF

2. The LCMM spatial discretizations

In the LCMM, spatial discretization is performed over non-uniformly distributed points. Each computational point is connected to a set of neighboring points, and this connectivity defines a local topology. The LCMM can handle the irregularly distributed points owing to two features of the localized meshless formulation: the radial basis function collocation and the polynomial expansion with MLS treatment.



Local topology: each point is associated with nearest NF points

2.1. The local topology build-up

Every point on the domain boundary and interior of the discretized geometry is identified as a data center that recruits a set of neighboring influence points to make up a localized interpolation topology. It is over this topology of points that the field variable is estimated using proper functions. For the LCMM considered in this paper, those functions consist of RBFs augmented by polynomials. The total number of points in the topology including the data center and the neighboring influence points is denoted by NF . For a two-dimensional (2D) geometry, the creation of the localized interpolation topology is accomplished by incrementally inflating a circle starting from the data center. In 3D, a corresponding sphere is expanded.

The circle is inflated until it encompasses a prescribed number of influence points. The number of influence points depends on whether the data center is on the boundary or in the interior. For the data centers on the boundary, the inflated circle is taken to encompass a minimum of 18 points in a 2D space. The build-up of a typical topology for a boundary data center in 2D is shown in Fig. 1(a). It is important to mention that the topology around any

.....

2.2. The localized RBF collocation

The value of a field variable, say ϕ , can be collocated at an arbitrary point i within the local topology by a RBF interpolation such as

$$\phi_i = \sum_{j=1}^{NF} \alpha_j \chi_j(\mathbf{x}_i) \tag{1}$$

Here, \mathbf{x}_i represents the Cartesian coordinates of the collocation point i . The terms α_j represent the unknown expansion coeffi-

This is Hardy multiquadrics radial base function

$$\chi_j(\mathbf{x}_i) = [r_j^2(\mathbf{x}_i) + c^2]^{n-(3/2)} \tag{2}$$

where n is a positive exponent parameter, c is a shape parameter, and $r_j(\mathbf{x}_i)$ is the Euclidean distance from (\mathbf{x}_i) to (\mathbf{x}_j) , which

MESHLESS

Moreover, to ensure that constant and linear fields are exactly captured, the RBF local interpolation expressed in Eq. (1) is completed by the addition of a polynomial. As such, the field variable at an arbitrary point i within the local topology can be recast such as

$$\phi_i = \sum_{j=1}^{NF} \alpha_j \chi_j(\mathbf{x}_i) + \sum_{j=1}^{NP^*} \alpha_{NF+j} P_j(x_i) \quad (8)$$

Incorporating completeness conditions in the collocation process leads to the augmented collocation matrix equation:

$$\begin{bmatrix} \chi_1(\mathbf{x}_1) & \dots & \chi_{NF}(\mathbf{x}_1) & P_1(\mathbf{x}_1) & \dots & P_{NP^*}(\mathbf{x}_1) \\ \vdots & & \vdots & \vdots & & \vdots \\ \chi_1(\mathbf{x}_{NF}) & \dots & \chi_{NF}(\mathbf{x}_{NF}) & P_1(\mathbf{x}_{NF}) & \dots & P_{NP^*}(\mathbf{x}_{NF}) \\ P_1(\mathbf{x}_1) & \dots & P_1(\mathbf{x}_{NF}) & 0 & \dots & 0 \\ \vdots & & \vdots & \vdots & & \vdots \\ P_{NP^*}(\mathbf{x}_1) & \dots & P_{NP^*}(\mathbf{x}_{NF}) & 0 & \dots & 0 \end{bmatrix} \times \begin{pmatrix} \alpha_1 \\ \vdots \\ \alpha_{NF} \\ \alpha_{NF+1} \\ \vdots \\ \alpha_{NF+NP^*} \end{pmatrix} = \begin{pmatrix} \phi_1 \\ \vdots \\ \phi_{NF} \\ 0 \\ \vdots \\ 0 \end{pmatrix} \quad (9)$$

The polynomial enrichment will subsequently take effect on the evaluation of the multiplication vector $\{\mathcal{L}\}$ that is expressed in Eq. (7), and this is a straightforward extension.

2.3. The polynomial MLS approximation

The value of the field variable ϕ can be alternatively approximated at an arbitrary point i within the local topology by the MLS-based polynomial interpolation. This is alternative manner to evaluate ϕ in addition to the local RBF collocation, and this approach is effective in determining one-sided derivatives that appear in the convective terms of the fluid flow momentum conservation equations. The approximated value of ϕ can be set to be equal to the multiplication of a polynomial basis vector P and a polynomial coefficients vector β . Each entry in P is a monomial and the total number of those entries is denoted by NP . The value of ϕ at an arbitrary point i within the local topology is approximated as

$$\hat{\phi}(x) = \sum_{j=1}^{NP} P_j(x) \beta_j \quad (10)$$

The polynomial basis vector can have as many entries as desired. For example, Eq. (11) shows a polynomial basis vector in a 2D Cartesian coordinate system, taken up to the first six entries of the Pascal triangle

$$P_j(x_i) = \begin{pmatrix} 1 \\ x \\ y \\ xy \\ x^2 \\ y^2 \end{pmatrix} \quad (11)$$

Increasing NP leads to a high-order approximation as well as to an increase in the computational cost. The number of points in the local topology NF should be at least equal to NP to avoid numerical instabilities.

A standard least squares fit is accomplished by first defining scalar measure, E , of the sum of the squares of the errors between the nodal value ϕ and the polynomial expansion approximation $\hat{\phi}$ at each point of the local topology as

$$E = \sum_{i=1}^{NF} (\phi_i - \hat{\phi}_i)^2 = \sum_{i=1}^{NF} \left(\phi_i - \sum_{j=1}^{NP} P_j(x_i) \beta_j \right)^2 \quad (12)$$

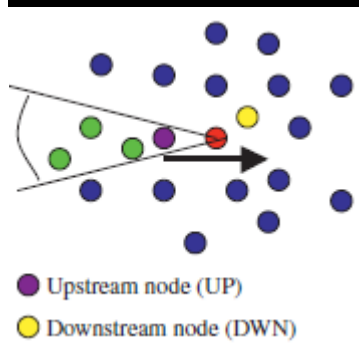
MESHLESS method EXAMPLE RBF

3. The LCMM upwinding technique

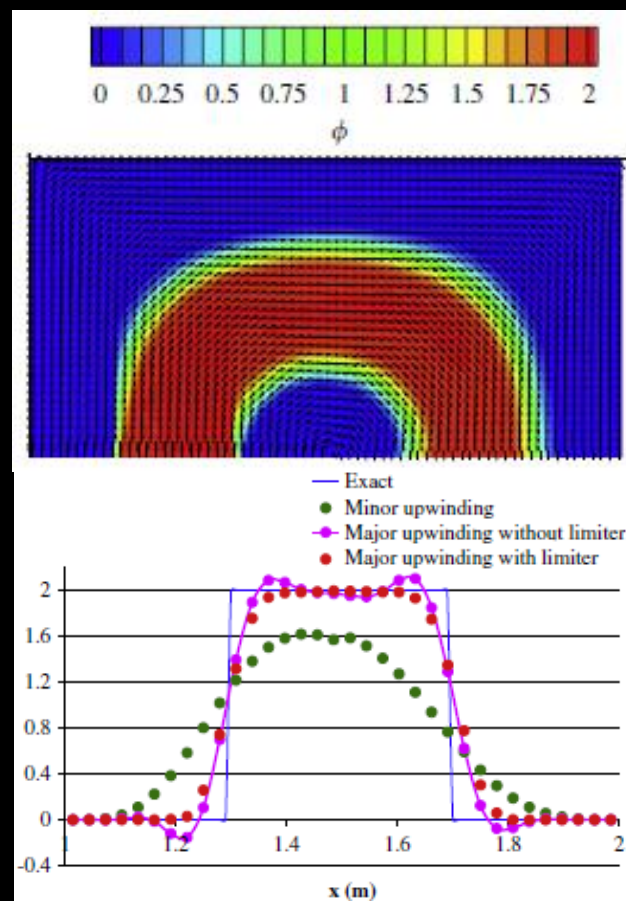
Evaluating the field variable first-order derivatives appearing in the convective terms of a given transport equation for convection-dominated transport problems requires special attention. For the numerical solution of any transport equation, an upwinding technique combined with a limiter becomes necessary when the convection effects acting in the flow stream-wise direction outweigh the diffusion effects [33,34]. For this purpose, we utilize a high-order upwinding scheme algorithm augmented with a limiter. Subsequently, one dimensional (1D) and 2D results are presented to illustrate the accuracy of the LCMM upwinding/limiter scheme.

3.1. The LCMM upwinding and limiter scheme

We refer to such a modified topology as the “upwinding topology”. In the upwinding topology, the data center is no longer at the center of the topology and the number of points is reduced from NF to NU . Instead of inflating a circle/sphere, a sector/cone is drawn from the data center upstream-wise to recruit upstream influence points that are indispensable for the upwinding process. The closest upstream point to the data center can be singled out of the upstream points and is referred to as the “close upstream point”; the rest of the upstream points will then be referred to as the “far upstream points”. Then, the data center recruits the closest downstream point as it adds more accuracy to the upwinding process. So after all, the upwinding topology will comprise the data center, the close upstream point, the far upstream points, and a single downstream point; the sum of all those points will be NU . A typical upwinding topology structure is shown in Fig. 5 for a uniform point distribution (a) and a non-uniform point distribution (b).



Benchmark-pure convection



CFD2 MESHLESS method EXAMPLE RBF

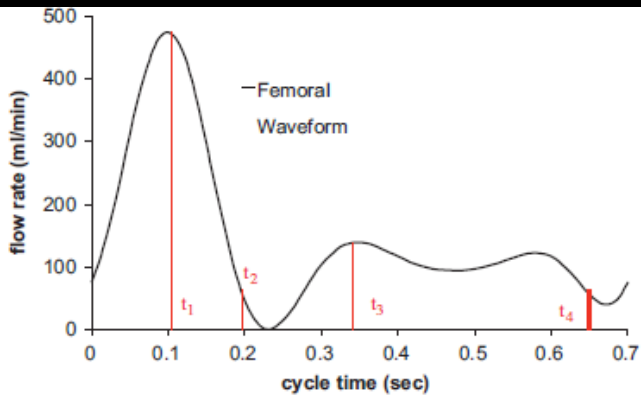


Fig. 22. The femoral flow waveform at the conventional ETSDA geometry inlet.

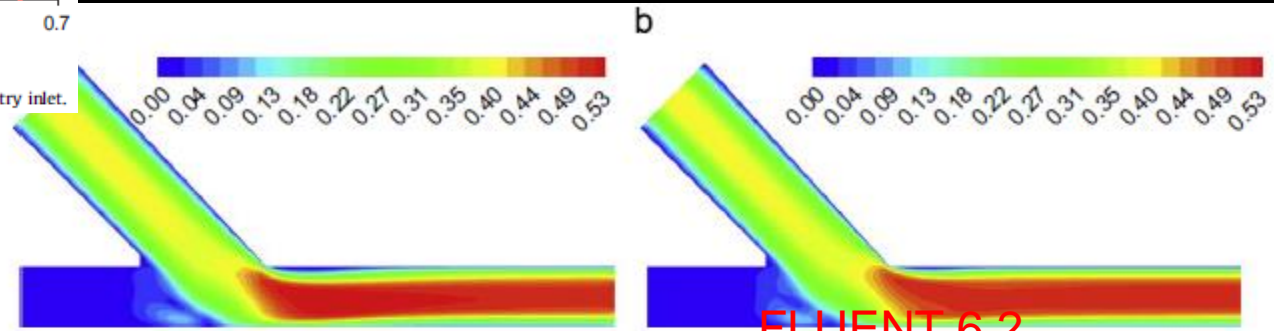


Fig. 23. Meshless (a) and FVM (b) velocity contours at t_1 with femoral flow.

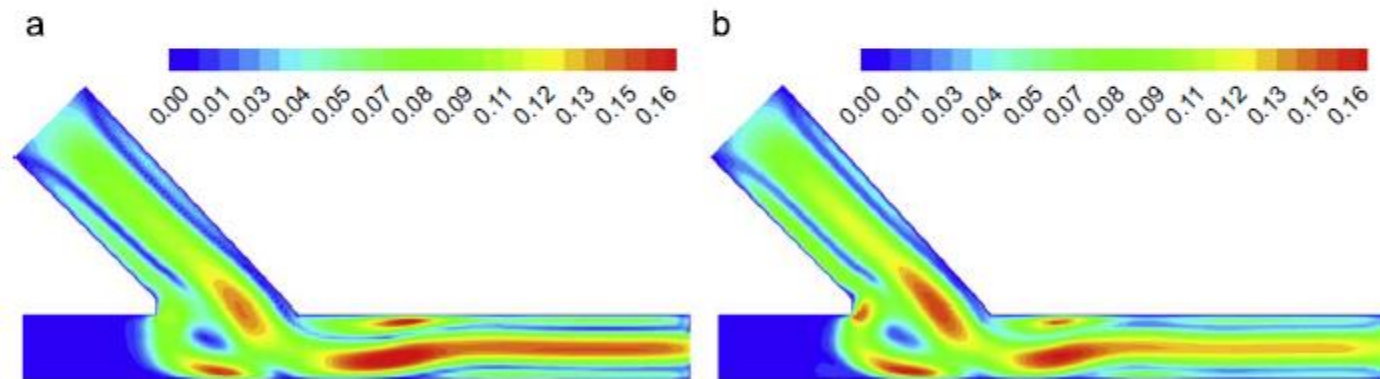




Fig. 24. Meshless (a) and FVM (b) velocity contours at t_2 with femoral flow.

MESHLESS Navier Stokes


Elsevier
500 articles on
Meshless
Navier Stokes


1  **Meshless schemes for unsteady Navier–Stokes equations in vorticity formulation using radial basis functions** Original Research Article
Journal of Computational and Applied Mathematics, Volume 192, Issue 2, 1 August 2006, Pages 328-338
Zhang Yun-Xin, Tan Yong-Ji
[Show preview](#) | [PDF \(196 K\)](#) | [Related articles](#) | [Related reference work articles](#)


2  **Meshless point collocation for the numerical solution of Navier–Stokes flow equations inside an evaporating sessile droplet** Original Research Article
Engineering Analysis with Boundary Elements, Volume 36, Issue 2, February 2012, Pages 240-247
G.C. Bourantas, A.J. Petsi, E.D. Skouras, V.N. Burganos
[Show preview](#) | [PDF \(656 K\)](#) | [Related articles](#) | [Related reference work articles](#)


Highlights


- The flow field inside an evaporating sessile droplet is computed with meshless numerical techniques.
- The Moving Least Squares and the Radial Basis Function approximations are employed.
- An augmented linear system to tackle the zero shear-stress condition at the interface is used.
- The results compare very satisfactorily with analytical and finite volume predictions.

3  **Collocated discrete least squares (CDLS) meshless method for the stream function-vorticity formulation of 2D incompressible Navier–Stokes equations** Original Research Article
Scientia Iranica, In Press, Uncorrected Proof, Available online 8 October 2012
M. Lashkarbolok, E. Jabbari
[Show preview](#) | [PDF \(2434 K\)](#) | [Related articles](#) | [Related reference work articles](#)

4  **Corrected discrete least-squares meshless method for simulating free surface flows** Original Research Article
Engineering Analysis with Boundary Elements, Volume 36, Issue 11, November 2012, Pages 1581-1594
G. Shobeyri, M.H. Afshar
[Show preview](#) | [PDF \(3073 K\)](#) | [Related articles](#) | [Related reference work articles](#)

5  **Meshless local Petrov–Galerkin method-higher Reynolds numbers fluid flow applications** Original Research Article
Engineering Analysis with Boundary Elements, Volume 36, Issue 11, November 2012, Pages 1671-1685
Mohammad Najafi, Ali Arefmanesh, Vali Enjilela
[Show preview](#) | [PDF \(3011 K\)](#) | [Related articles](#) | [Related reference work articles](#)

6  **The method of fundamental solutions for solving incompressible Navier–Stokes problems** Original Research Article
Engineering Analysis with Boundary Elements, Volume 33, Issues 8–9, August–September 2009, Pages 1031-1044
D.L. Young, Y.C. Lin, C.M. Fan, C.L. Chiu
[Show preview](#) | [PDF \(1164 K\)](#) | [Related articles](#) | [Related reference work articles](#)

7  **Development of a meshless Galerkin boundary node method for viscous fluid flows** Original Research Article
Mathematics and Computers in Simulation, Volume 82, Issue 2, October 2011, Pages 258-280
Xiaolin Li
[Show preview](#) | [PDF \(2113 K\)](#) | [Related articles](#) | [Related reference work articles](#)